Journal of Analytical and Applied Pyrolysis 105 (2014) 83–90

Contents lists available at ScienceDirect

Journal of Analytical and Applied Pyrolysis

journal homepage: www.elsevier.com/locate/jaap

# Synthetic fuel production from cottonseed: Fast pyrolysis and a TGA/FT-IR/MS study

Esin Apaydin-Varol[a,*], Başak Burcu Uzun[a], Eylem Önal[b], Ayşe E. Pütün[a]

[a] Anadolu University, Department of Chemical Engineering, Eskisehir, Turkey
[b] Bilecik Şeyh Edebali University, Department of Chemical and Processing Engineering, Bilecik, Turkey

ARTICLE INFO

*Article history:*
Received 20 May 2013
Accepted 16 October 2013
Available online 24 October 2013

*Keywords:*
Fast pyrolysis
TGA-FTIR-MS
Cottonseed
Bio-oil

ABSTRACT

This study investigates the thermal decomposition behavior of cottonseed via TGA/FT-IR/MS and the quantification/characterization of liquid products from fast pyrolysis. Thermal degradation of the biomass sample has occurred in four steps, corresponding to the removal of moisture, decomposition of cellulose, hemicellulose and lignin and it was completed at about 700 °C. The main gaseous products evolved were $CO_2$, light hydrocarbons and $H_2O$. For the fast pyrolysis experiments, particular investigated process variables were temperature (400–700 °C), heating rate (5–700 $^\circ C\,min^{-1}$) and nitrogen gas flow rate (100–800 $cm^3\,min^{-1}$). Maximum oil yield was attained at 500 °C with a yield of 49.5% under 200 $cm^3\,min^{-1}$ nitrogen flow rate and at a heating rate of 300 $^\circ C\,min^{-1}$. Bio-oil obtained at optimum conditions are separated into its fractions by column chromatography. The oil and its sub-fractions were characterized by elemental analysis, FT-IR, and GC/MS. The char was characterized with elemental analysis and FT-IR techniques. The aliphatic sub-fraction of the obtained bio-oil contains predominantly straight chain of n-alkanes and alkenes. According to the chemical characterization, the bio-oil can be utilized as conventional liquid fuels.

## 1. Introduction

Today, most of the energy requirements of the developing countries are provided by petroleum-related products. The scarcity of conventional fuels, growing emissions of combustion generating pollutants and their increasing costs will make biomass as a clean and renewable substitute for fossil fuels and it seems to be the most promising source for producing economically competitive liquid transportation oils [1–4]. Fast pyrolysis of biomass is a leading method for producing bio-oil which is the preferred product due to its great potential as transport fuels and various advantages such as low cost, high thermal efficiency, high calorific value, low $CO_2$, $SO_x$ and $NO_x$ emissions [5,6].

Turkey is a producer, processor and exporter of cotton (*Gossypium hirsitum*) and its products. The cotton plant is mainly composed of fiber (35–40%) and seed (60%). Although cotton is being cultivated mainly for its fiber for textile industry, its seed is an important raw material for oil production. However, particularly low rates of seed oil content (17–24%) leads to the presence of a limited production of edible cottonseed oil. Cotton is one of the most important agricultural crops in Turkey. In 2011, cottonseed production was estimated as 1.5 million tones with a yield of 282 kg/hectare. Due to having high calorific value, bio-fuel can be produced from the oil seeds via pyrolysis, liquefaction or transesterification [7,8].

In the past decade, transesterification of cottonseed oil has generated significant interest [9–11]. However, this method mainly consists of extraction, methanolysis and purification steps that are time consuming and require expensive chemicals. Being a one-step-easy thermochemical conversion method, fast pyrolysis seems to be an advantageous method for synthetic fuel production [12,13]. The bio-oil obtained from fast pyrolysis is typically a complex mixture of oxygenated hydrocarbons with lower nitrogen and sulfur compounds and therefore it can be used as a substitute for fossil fuel for power generation or production of value added chemicals [14]. In this context, this study covers the fast pyrolysis of cottonseed under different conditions to investigate the proper one to produce bio-oil with a high yield.

Many researchers have investigated the potential recovery of fuels and chemicals from biomass and vegetable oils via pyrolysis in relation to process conditions. Oil from soybean [15], palm tree [16], castor [17], and canola [18] were selected as raw materials for the production of diesel-like biofuels via pyrolysis. The characterization of gas and liquid products were reported in these studies and the formation of linear and cyclic paraffins, olefins, aldehydes, ketones, and carboxylic acids were observed during thermal decomposition [17]. The compositions of gaseous hydrocarbon and gasoline produced through pyrolysis of cottonseed oil with both equilibrium catalysts and silica sand was investigated in

---

[*] Corresponding author. Tel.: +90 222 33350580/6516; fax: +90 222 3239501.
*E-mail address:* eapaydin@anadolu.edu.tr (E. Apaydin-Varol).

0165-2370/$ – see front matter © 2013 Elsevier B.V. All rights reserved.
http://dx.doi.org/10.1016/j.jaap.2013.10.006

another study [19]. It was reported that reaction products such as dry gas, liquefied petroleum gas and gasoline are heavily dependent on the catalyst type and reaction conditions. Özbay et al. [20] studied cottonseed cake pyrolysis to determine the effects of reactor geometry, pyrolysis atmosphere and pyrolysis temperature on the product yields and chemical composition of the liquid product. The maximum oil yield was attained under nitrogen atmosphere at a pyrolysis temperature of 550 °C with a heating rate of 7 °C $\mathrm{min}^{-1}$ in tubular reactor. Cottonseed cake pyrolysis was also studied by Putun et al. [21] and the maximum oil yield was obtained as 24% under static retort atmosphere whereas it reached a value of 29.68% under $N_2$ atmosphere. They have reported the catalytic pyrolysis of cottonseed cake by selecting natural zeolite as the catalyst under static and nitrogen atmospheres to investigate the effect of catalyst–biomass ratio on product yields at 550 °C. The maximum liquid yield obtained was 30.84% in the presence of natural zeolite (20 wt.% of raw material) with a sweeping gas flow rate of 100 mL $\mathrm{min}^{-1}$. In another work of Pütün [22], cottonseed is pyrolyzed in a tubular fixed-bed reactor under various sweeping gas ($N_2$) flow rates at different pyrolysis temperatures with or without catalyst (MgO) addition. In the non-catalytic work, they obtained the maximum bio-oil yield as 48.30% at 550 °C with a sweeping gas flow rate of 200 mL $\mathrm{min}^{-1}$. It was found that catalyst addition decreased the quantity of bio-oil, yet increased the quality of bio-oil in terms of calorific value, hydrocarbon distribution and removal of oxygenated groups.

According to literature review, it is reported that pyrolysis conditions and thermal decomposition behavior of the selected biomass sample have great influences on product yields. Application of thermogravimetric analysis (TGA) is a common technique that is widely used to figure out the thermal decomposition behavior and to study chemical kinetics of complex reactions occurring as a result of pyrolysis of various biomass samples [23–28]. Recently, the combination of TGA with Fourier Transform Infrared Spectrometer (FT-IR) and Mass Spectrometer (MS) attracts attention for both the determination of thermal degradation profiles and the detection of evolved gases during pyrolysis [29]. In literature there are some studies including TGA-FTIR-MS analysis for biomass samples such as lignin from prairie cord grass [27], pine wood waste [30], cotton stalk [31]. On the other hand, there is limited information about TGA-FTIR-MS analysis of cottonseed.

The objective of the present work is to produce bio-fuel from cottonseed via thermal decomposition instead of using multi-step methods and to optimize the bio-oil yield by changing different parameters such as pyrolysis temperature, heating rate and nitrogen gas flow rate in a fixed bed tubular reactor. This paper also presents the thermal decomposition behavior of cottonseed using TGA-FTIR-MS to analyze the evolved gases. Furthermore, the characterization of bio-oil obtained under appropriate conditions from fast pyrolysis was investigated using column chromatography, elemental analysis, FT-IR and GC/MS for composition.

## 2. Materials and methods

### 2.1. Properties of raw material

The cottonseed sample investigated in this study has been taken from a farm around Antalya located in Mediterranean Sea region in Southern part of Turkey. Prior to use, the sample was air-dried and ground in a high-speed rotary cutting mill. The results for proximate and component immiscible that were applied to the ground, air dried cottonseed samples having average particle size of 0.92 mm were given in Table 1. The feedstock moisture was found to be as 4.61 wt.%. Low ash content of cottonseed makes it favorable as a raw material, when compared with conventional fuels [32]. The raw material consists of 29.29% hollocellulose, 14.29% lignin and a significant amount of n-hexane solubles (17.00 wt.%). Ultimate analysis was performed on cottonseed samples to determine the elemental composition. With the known values of C, H, N, S and O weight percentages and using Du-Long's equation calorific value of the raw material was calculated as 25.82 MJ $\mathrm{kg}^{-1}$ [32].

**Table 1**
Properties of cottonseed (wt.%).

| | % |
|---|---|
| Moisture | 4.61 |
| Ash | 3.31 |
| Volatile matter | 79.47 |
| Fixed carbon | 12.61 |
| Holocellulose | 29.29 |
| Lignin | 14.29 |
| Oil | 17.00 |
| Elemental composition | |
| C | 55.41 |
| H | 8.82 |
| N | 4.41 |
| O (by difference) | 31.36 |
| Calorific value (MJ/kg) | 25.82 |

Thermal decomposition of cottonseed was studied with a Setaram Labsys Thermogravimetric Analyser (TGA) coupled with FT-IR (Thermo Nicolet IZ 10) and MS (Pfeiffer Omni Star). Simultaneous measurements were carried out using 100 μL $Al_2O_3$ crucibles without lids in order to get the best possible heat transfer between the thermocouples and crucibles. 10 ± 0.5 mg of sample was heated to the final temperature of 1000 °C with a heating rate of 10 °C $\mathrm{min}^{-1}$ and nitrogen flow rate of 20 mL $\mathrm{min}^{-1}$. FT-IR was used for evolved gases analysis in the range of 4000–400 $\mathrm{cm}^{-1}$, and hence the transfer line and gas cell was kept at constant temperatures of 225 and 250 °C to avoid condensation and secondary reactions. For MS analysis evolved gases were scanned simultaneously for the selected $m/z$ values. The capillary transfer line was kept at 190 °C and a Faraday type detector was used for multiple ion detection (MID) scanning.

### 2.2. Pyrolysis experiments

For the determination of optimum conditions to convert biomass to biofuels via thermal decomposition, three sets of experiments were performed using a tubular reactor details of which were given in one of our previous studies [33]. The 316 stainless steel tubular reactor was 90 cm in height and has 2.5 cm internal diameter. Sweeping gas (nitrogen) was introduced at the top of the reactor and its flow rate was adjusted with a rotameter. Heating rate and pyrolysis temperature were controlled with a PID controller.

First set of experiments was performed to determine the effect of the pyrolysis temperature on product yields. 5 g of air-dried sample was placed into the reactor and a sweeping gas flow rate of 200 $\mathrm{cm}^3\,\mathrm{min}^{-1}$ was controlled and measured with a rotameter. The sample was heated with a heating rate of 300 °C $\mathrm{min}^{-1}$ up to the selected final pyrolysis temperatures of either 400, 500, 550, 600, 700 °C and held at that temperature for 10 min. The second group of experiment was established to see the effect of heating rate on the pyrolysis yields. These experiments were conducted with five different heating rates (5, 100, 300, 500, 700 °C $\mathrm{min}^{-1}$) at a constant pyrolysis temperature of 500 °C and sweeping gas flow rate of 200 $\mathrm{cm}^3\,\mathrm{min}^{-1}$. The last group of experiments was performed to determine the effect of sweeping gas flow rate on bio-oil yield by taking into account the highest oil yields of the previous experiments. Therefore, the experiments were carried out to the final temperature of 500 °C with a heating rate of 300 °C $\mathrm{min}^{-1}$ and a sweeping gas flow rate of either 100, 200, 400 or 800 $\mathrm{cm}^3\,\mathrm{min}^{-1}$. The volatile products obtained during thermal decomposition passed through three traps, which were kept at about 0 °C using an ice bath. The total liquid product including bio-oil and water was condensed in ice cooled traps and recovered with dichloromethane (DCM). Condensed water was formed not only as a result of the pyrolysis reactions but as a result of condensation of moisture in the raw material. Water and bio-oil dissolved in DCM are immiscible and hence they can be separated easily by a separation funnel. The bio-oil and solvent mixture was passed over anhydrous sodium sulfate to make it water free and then the solvent was removed in a rotary evaporator. The residual solid in the reactor was weighed as char. The gas yield was calculated by taking the difference. In this study, all the yields were expressed on a dry and ash-free basis, and their values were taken as the average of at least three experiments with an experimental error of ±5%.

### 2.3. *Characterization*

Bio-oil obtained at the final temperature that gave maximum oil yield was selected for characterization. The elemental composition and calorific value of the bio-oil was determined by Carlo Erba 1108 Elemental Analyzer and Du-Long's equation, respectively. Liquid column chromatography was applied to classify bio-oil into its subfractions. 1.0 ± 0.1 g of bio-oil was first separated into n-pentane soluble and insoluble compounds (asphaltenes), of which the n-pentane soluble compounds were further separated by adsorption chromatography. The column used was packed with silica gel 70–230 mesh that was pre-treated at 600 °C for 8 h prior to use. The column that is 1.5 cm in diameter and 100 cm length was filled with silica gel up to ¾ of the total volume. n-Pentane soluble fraction was then eluated successively with 200 mL of n-pentane, toluene and methanol to produce aliphatic, aromatic, and polar subfractions, respectively. Solvents of each fraction were removed by rotary evaporator and sub-fractions were dried and weighed. The FT-IR spectra of the oils and their aliphatic, aromatic and polar subfractions were recorded using a Bruker Tensor 27 Model Fourier Transform Infrared Spectrometer. GC/MS analysis of the bio-oil and its aliphatic subfraction was performed using a Hewlett–Packard 6890 Model gas chromatograph equipped with a 5973 mass selective detector using HP 5-MS column by injecting 1 μL of sample manually. For bio-oil analysis heating program was applied as follows: 3 minutes waiting at 40 °C, heating with a rate of 2 °C $\text{min}^{-1}$ till 280 °C. The mass spectrometer was operated in a mass range of 0–300 amu. Interpretation of the compounds in the bio-oil and its subfraction was tentatively made according to the results of on an automatic library search (Wiley 275).

## 3. Results and discussion

Thermal decomposition of cottonseed was examined between room temperature and 1000 °C under inert atmosphere to investigate the degradation behavior and the composition of evolved gases with the help of FT-IR and MS that were connected to TGA. On the other hand, pyrolysis was carried out in three groups of experiments to investigate the effect of pyrolysis conditions on the product yields and to determine the pyrolysis conditions giving the maximum bio-oil yield.

### 3.1. *Thermal decomposition of cottonseed*

TG and dTG curves for cottonseed is given in Fig. 1(a). From dTG curve there can be seen four peaks at the different temperature ranges. The first peak, around 90 °C, is obviously responsible for the moisture retained in the biomass. The following three peaks are due to main decomposition reactions indicating the presence of three major biomass constituents, namely hemicellulose, cellulose and lignin and as well as the presence of significant amount of oil in the cottonseed. The temperature at which decomposition appears to start and end, and also shape of the curve depend upon many factors such as heating rate, pyrolysis atmosphere, particle size, initial amount and type of the biomass selected. It can be seen from Fig. 1(a) that main decomposition with a weight loss of 71.3% takes place between 157 and 553 °C and reaches a flat platform around 700 °C. The first derivative of the TG curve (dTG) shows three decomposition steps with the maximum temperatures of 266.23, 338.17, 392.63 °C and this indicates that maximum decomposition ends around 400 °C. According to this data, pyrolysis temperature is selected between 400 and 700 °C for the tubular reactor experiments.

During the thermal decomposition of cottonseed under inert atmosphere, evolved gases were detected via FT-IR and MS. Both analysis methods are found to be in a consistency with each other and the mass loss curve obtained from TGA. It is obvious from Fig. 1(b) that when pyrolytic reactions start at about 200 °C, related products such as $CO_2$, CO, $CH_4$, $H_2O$, ketones, aldehydes, acids and other hydrocarbons are formed. Three dimensional FT-IR data shows that C=O stretching vibrations related with $CO_2$ (band between 2210 and 2400 $\text{cm}^{-1}$) has its maximum at 345 °C whereas C—H stretching vibration band (2840–3061 $\text{cm}^{-1}$), assigned to the presence of hydrocarbon gases mainly $CH_4$, has its maximum absorbance at 460 °C. $H_2O$ peaks (O—H stretching vibration band between 3100 and 3500 $\text{cm}^{-1}$) are seen in two sections indicating (i) the moisture release from the biomass (temperatures between 85 and 140 °C) and (ii) water formed as a result of many parallel and consecutive reactions (temperatures between 185 and 330 °C). Carbonyl and C=C stretch vibration bands seen between 1850 and 1690 $\text{cm}^{-1}$ have two maximum peaks at temperatures of 290 and 353 °C indicating the release of aldehydes and acids.

Functional group information about the evolved gases during pyrolysis can be detected via FT-IR. However, mass spectroscopy has an important role on the determination of exact composition. Single ion current curves for the pyrolysis products obtained during the heating process are given in Fig. 1(c). It can be observed from the figure that intensive signals of the evolved gases appear within the temperature range of 187 and 523 °C being in a consistency with TGA measurements. Mass to charge ratio ($m/z$) of 44 is related with carbon dioxide and its maximum value is obtained at 330 °C. Formation of methane can be confirmed by the $m/z$ 16 and its peak in Fig. 1 starts at 216 °C where pyrolytic reactions mainly due to the decomposition of cellulose and hemicellulose start. The formation of hydrocarbon gases such as $C_2H_5$ and CHO ($m/z = 29$), $C_3H_5$ ($m/z = 41$), $C_3H_6$ and $C_2H_2O$ ($m/z = 42$), $C_3H_7$ and $CH_3CO$ ($m/z = 43$) can be also identified from MS data.

### 3.2. *Effect of pyrolysis temperature on product yields*

Pyrolysis temperature plays an important role on product distribution. According to previous studies with different biomass samples, it can be concluded that relatively low pyrolysis temperatures around 400 °C favor char formation, temperatures up to 600 °C maximize the production of bio-oils and temperatures above 700 °C maximize gaseous products while minimizing char formation [34–37].

In this study, to determine the effect of pyrolysis temperature on pyrolysis products yields, the experiments were conducted with a heating rate of 300 °C $\text{min}^{-1}$, sweeping gas flow rate of 200 $\text{cm}^3\,\text{min}^{-1}$ and at final temperatures of 400, 500, 550, 600, 700 °C. Results of the experiments are given in Fig. 2. As can be seen, the char yield decreased from 31.20 to 18.60%, as the final pyrolysis temperature was raised from 400 to 700 °C. On the contrary, gas yield increased from 16.70 to 38.40% with the same temperature increase. While the oil yield was 39.7% at the pyrolysis temperature of 400 °C, it appeared to go through a maximum of 49.5% at the final

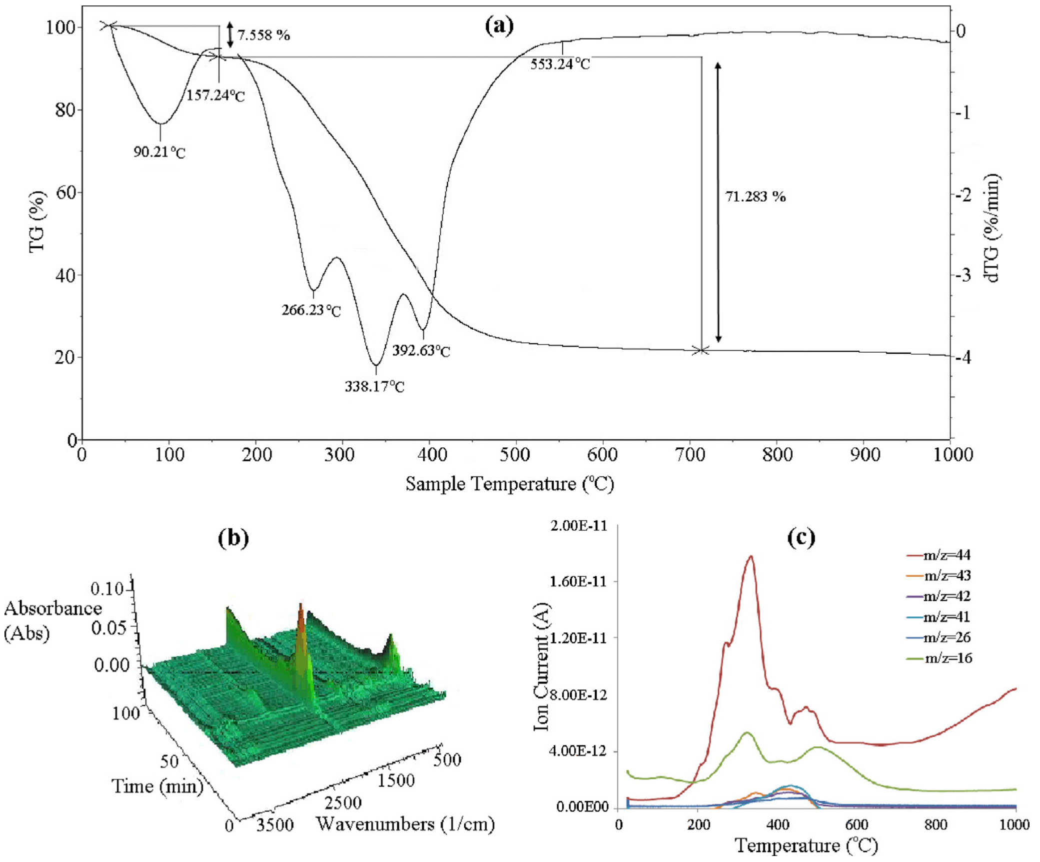

**Fig. 1.** TGA-FTIR-MS graphs for the thermal degradation of cottonseed (a) TG–dTG curves (b) 3d FT-IR spectra, (c) single ion current curves for the selected fragments.

temperature of 500 °C. Then at the final pyrolysis temperature of 700 °C, the oil yield decreased to 29.3%.

According to results from TGA experiments, the evolution of volatiles ends at about 553 °C at which bio-oil yield starts decreasing in the tubular reactor. Two important peaks are observed for $CH_4$ and $CO_2$ in the TGA-MS data (Fig. 1(c)), the first one being at 338 °C, and the second one at 483 °C indicating that selecting optimum pyrolysis temperature for the tubular reactor experiments as 500 °C is in consistency with instrumental data.

### 3.3. *Effect of heating rate on product yields*

Slow pyrolysis, being the conventional one, favors char formation, whereas fast pyrolysis is preferred when bio-oil is the target product. It is known that the yield of volatile matter increases with increasing heating rate. The higher the heating rate, the less time is available for tar cracking and consequently the more tar and less char produced. Indeed, reduced heat and mass transfer limitations result in higher oil yields at higher heating rates [12].

Fig. 3 shows the results of the second group of experiments that were performed to distinguish the difference between slow and fast pyrolysis on product yields. Referring the first set of experiments, pyrolysis temperature was chosen as 500 °C and nitrogen gas flow rate was kept at 200 $cm^3 min^{-1}$ during these experiments. As expected, higher heating rates minimized char yields. For slow pyrolysis (at 5 °C $min^{-1}$) bio-oil yield was achieved as 39.40% and with an increase of about 26%, it reached its maximum value at 300 °C $min^{-1}$. Then, at the higher heating rates bio-oil yield showed a decreasing tendency till to 41.80% at 700 °C $min^{-1}$. Increasing the heating rate from 5 to 700 °C $min^{-1}$ caused a reduction of char

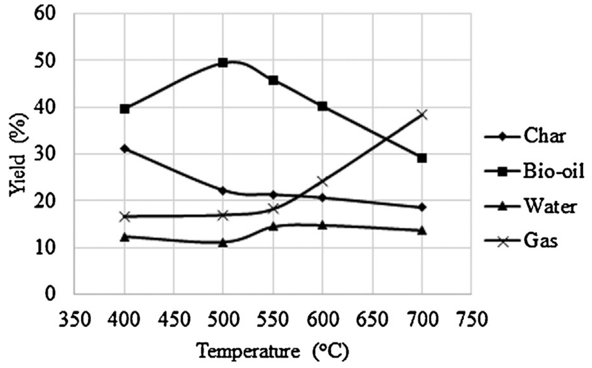

**Fig. 2.** Effect of pyrolysis temperature on product yields (heating rate: 300 °C $min^{-1}$; $N_2$ flow rate: 200 $cm^3 min^{-1}$).

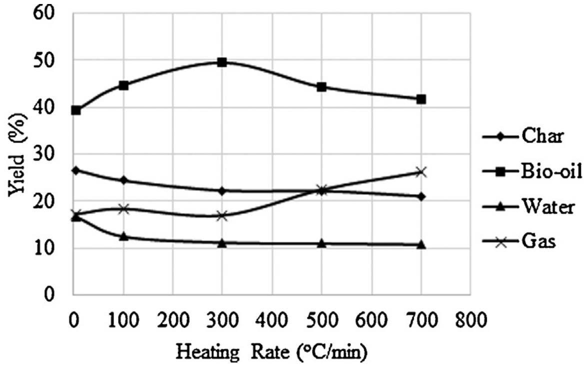

**Fig. 3.** Effect of heating rate on product yields (pyrolysis temperature: 500 °C; $N_2$ flow rate: 200 $cm^3 min^{-1}$).

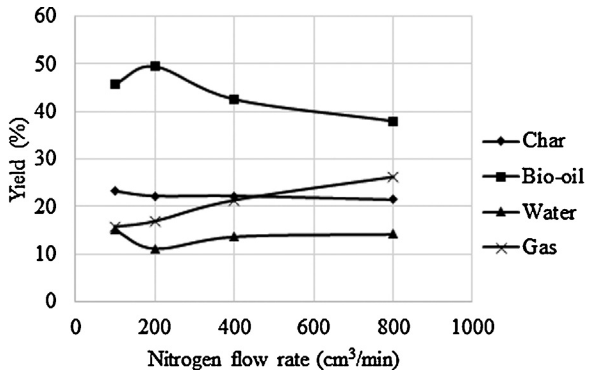

**Fig. 4.** Effect of nitrogen gas flow rate on product yields (pyrolysis temperature: 500 °C; heating rate: 300 °C min$^{-1}$).

yields from 26.60 to 21.10% and an increase of gas yields from 17.30 to 26.70%.

### 3.4. *Effect of sweeping gas flow rate on product yields*

The pyrolysis atmosphere can affect both the quantity and quality of all products. The use of inert gases is one of the major interest in tubular reactors used in this type of processes as predicted in literature. In addition, nitrogen flow influence the residence time of the vapour phase produced by pyrolysis and prevents the secondary cracking reactions at vapour phase [35].

Sweeping gas flow rates of 100, 200, 400 and 800 cm$^3$ min$^{-1}$ were tested on the cottonseed samples with a heating rate of 300 °C min$^{-1}$ based on the second group of experiments. The product yields of pyrolysis in relation to flow rate of sweeping gas are given in Fig. 4. The bio-oil yield achieved at 100 cm$^3$ min$^{-1}$ nitrogen flow as 45.80%, reached a maximum value of 49.50%, when nitrogen flow rate was 200 cm$^3$ min$^{-1}$. However, the further increase in nitrogen flow rate reduced bio-oil yield. This unexpected decrease could be explained by insufficient quenching during experiments. Higher flow rates of sweeping gas caused short residence time for pyrolytic vapors in the reactor leading maximum bio-oil yields. Without a perfect quenching of thermally cracked pyrolysis vapors, it could not be possible to reach higher bio-oil yields. As the residence times are getting longer, secondary reactions such as dehydration, decarboxylation and condensation will occur that are responsible for higher char yields [35–37].

### 3.5. *Characterization of bio-oil*

Pyrolytic oils are complex mixtures consisting of organic compounds from wide variety of chemical groups. They are in acidic character within a pH range of 2.5 and 4.5 depending on the raw material and pyrolysis conditions [38]. To characterize the pyrolytic oil obtained at optimum conditions (temperature: 500 °C, heating rate: 300 °C min$^{-1}$, $N_2$ flow rate: 200 cm$^3$ min$^{-1}$), it was separated into two fractions: n-pentane soluble and insolubles. The n-pentane soluble material was further separated into three fractions; aliphatics, aromatics and polars by adsorption chromatography. The results of the adsorption chromatography showed that the pyrolysis oil consists of 67% n-pentane solubles (maltenes) and the rest is asphaltenes. The aliphatic, aromatic, and polar fractions of maltenes were 27.3, 26.3, and 46.4%, respectively.

The elemental compositions of bio-oil and its subfractions are given in Table 2. As can be seen, carbon and hydrogen contents of cottonseed bio-oil are higher than those of raw material. The average chemical composition of the fast pyrolysis oil is $CH_{1.88}N_{0.07}O_{0.1}$. The significant decrease in oxygen content of the oil compared to the original feedstock is important, because the high oxygen content is not attractive for the production of transportation fuels. The bio-oils from biomass usually contain higher proportion of oxygen than fossil oil, and thus they are quite reactive and not as stable as fossil fuels and their characteristics change rapidly during condensation and under storage conditions. Their utilization as fuels or sources of chemical feedstock requires some form of upgrading to improve storage stability and heating value. As the bio-oil from cottonseed has lower content of oxygen, it is more stable. And also, almost free of sulfur of the bio-oil is quite promising for its evaluation as fuel from environmental perspectives. On the other hand, cottonseed contains upto 25 wt.% protein and the presence of protein results in a higher nitrogen content in bio-oil and polar subfraction [39]. As seen, aliphatic sub-fraction contains no oxygen with a high amount of hydrogen content. Moreover, H/C ratio of bio-oil and aliphatic sub-fraction are 1.88 and 1.86 respectively, which are very close to that of gasoline [35].

The fast pyrolysis of biomass is complicated since the decomposition represents a large number of reactions in parallel and series. Different kinds of biomass possess different reactions in pyrolytic process, which caused the complexity and variation in the compositions of their bio-oils. Although bio-oils have various compositions, one of the key properties of bio-oils for use as a diesel substitute is its heating value [40]. Calorific value of raw material, bio-oil and its chromatographic subfractions are given in Tables 1 and 2. When calorific values of raw material and oil are compared, it can be seen that fast pyrolysis of raw material provided better quality oil with higher calorific value and H/C ratio. The heating value of bio-oil was 39.49 MJ kg$^{-1}$. This calorific value indicates that the energy content of bio-oil was very close to those of the conventional liquid fuels such as 45.18 MJ kg$^{-1}$ for diesel and 42–43 MJ kg$^{-1}$ for heavy fuel oil [41,42]. Owing to its high calorific value, the bio-oil can be utilized as fuels for various combustion systems in industry [43].

FT-IR is informative in the assignment of various functional groups. Biomass pyrolysis oils contain a very wide range of complex organic chemicals [44]. Results of FT-IR spectra of raw material, bio-oil and its subfractions are shown in Table 3 and Fig. 5. The

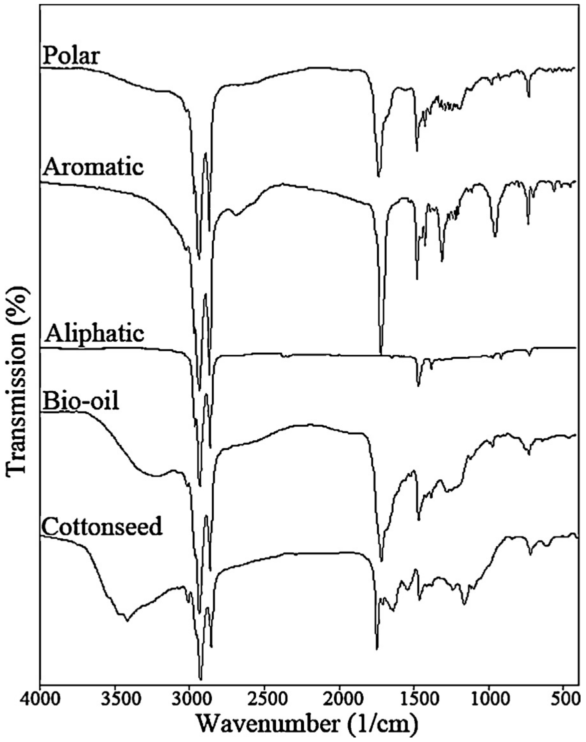

**Fig. 5.** FT-IR spectra of raw material, bio-oil and its subfractions.

**Table 2**
Elemental analysis results of the products (wt.%) and their empirical formulas (pyrolysis temperature: 500 °C; heating rate: 300 °C $\min^{-1}$; $N_2$ flow rate: 200 $cm^3 \min^{-1}$).

| Component | Bio-oil | Aliphatics | Aromatics | Polars |
|---|---|---|---|---|
| C | 72.92 | 86.45 | 78.52 | 75.11 |
| H | 11.48 | 13.37 | 13.77 | 12.54 |
| N | 5.92 | 0.18 | 0.10 | 3.02 |
| O (by difference) | 9.68 | 0.000 | 7.61 | 9.33 |
| Empirical formula | $CH_{1.88}N_{0.07}O_{0.10}$ | $CH_{1.86}N_{0.002}$ | $CH_{2.1}N_{0.001}O_{0.073}$ | $CH_2N_{0.034}O_{0.094}$ |
| Calorific value (MJ/kg) | 39.49 | 48.54 | 45.07 | 41.81 |

**Table 3**
Results of FT-IR spectra for raw material, bio-oil and its subfractions (pyrolysis temperature: 500 °C; heating rate: 300 °C $\min^{-1}$; $N_2$ flow rate: 200 $cm^3 \min^{-1}$).

| Type of functional group | Wavenumber ($cm^{-1}$) | Biomass | Bio-oil | Aliphatic fraction | Aromatic fraction | Polar fraction |
|---|---|---|---|---|---|---|
| OH stretch | 3150–3500 | 3414 | 3207 | – | – | – |
| Aromatic ring stretching | 3095–3016 | – | – | – | – | – |
| $\upsilon_{as}$[a] | 2955–2885 | 2926 | 2926 | 2924 | 2919<br>2954 | 2922 |
| $\upsilon_s$[b] | 2885–2845 | 2855 | 2855 | 2856 | 2850 | 2852 |
| C=C stretch | 1700–1400 | 1465<br>1545<br>1639 | 1413<br>1464<br>1515 | 1465 | 1411<br>1464 | 1413<br>1465<br>1546 |
| Ketone bending | 1715–1680 | 1711 | 1711 | – | 1707 | – |
| $\delta_{as}$[c] | 1474–1465 | – | – | – | – | – |
| $\delta_s$[d] | 1389–1374 | – | 1378 | 1378 | 1377 | 1380 |
| C—O ethers stretching | 1264–1245 | – | – | – | – | 1251 |
| Bending vibration band of carbonyl groups | 1172–1100 | 1163 | – | – | – | 1118 |

[a] Asymmetrical C—H stretching vibration of aliphatic $CH_3$ and $CH_2$.
[b] Symmetrical C—H stretching vibration of aliphatic $CH_3$ and $CH_2$.
[c] Scissoring bending vibration of aliphatic $CH_2$.
[d] Symmetrical C—H bending vibration of aliphatic $CH_3$.

O—H stretching vibrations between 3200 and 3400 $cm^{-1}$ indicate the presence of phenols and alcohols. Fig. 5 shows that no peak exists between these wave numbers for the aliphatic sub-fraction of bio-oil, and this indicates that aliphatic sub-fraction does not contain oxygenated compounds, and this result obtained in the present study was also in a consistency with the results of elemental and GC/MS analyses. The C—H stretching vibrations between 2850 and 2925 $cm^{-1}$ and C—H deformation vibrations between 1410 and 1515 $cm^{-1}$ indicate the presence of alkanes. Moreover, the location of bending vibration of C—H groups at 1378 $cm^{-1}$ provides another evidence of the fact that this band is very important for the detection of methyl groups in a given compound. Carbonyl stretching absorptions cause the band at about 1710 $cm^{-1}$ in the spectrum. These include primary, secondary and tertiary alcohols such as methanol, propanol, butanol and furfuryl alcohols, carboxylic acids, for example; formic, acetic, propionic, benzoic hexadecanoic and octadecanoic acids and their derivatives, ketones and aldehydes including acetaldehyde, benzadehyds,

**Table 4**
Tentative identification of bio-oil compounds by GC–MS (pyrolysis temperature: 500 °C; heating rate: 300 °C $\min^{-1}$; $N_2$ flow rate: 200 $cm^3 \min^{-1}$).

| Peak number | Retention time (min) | Product | Relative area (%) |
|---|---|---|---|
| 1 | 4.48 | Toluene | 1.93 |
| 2 | 7.66 | 2-Furanmethanol | 1.31 |
| 3 | 14.77 | Phenol | 1.56 |
| 4 | 17.41 | Corylone | 1.55 |
| 5 | 20.97 | 4-Methyl phenol | 3.21 |
| 6 | 21.55 | 2-Methoxy phenol | 0.75 |
| 7 | 26.17 | Pentyl-benzene | 1.08 |
| 8 | 29.64 | 1,2-Benzenediol | 2.89 |
| 9 | 33.13 | 3-Methoxy-1,2-benzenediol | 0.82 |
| 10 | 35.28 | 1H-indole | 1.02 |
| 11 | 36.71 | 4-Vinyl-2-methoxy phenol | 0.93 |
| 12 | 39.23 | 2,6-Dimethoxy phenol | 1.53 |
| 13 | 41.99 | Cyclododecane | 0.89 |
| 14 | 45.23 | 2-Methoxy-4-(2-propenyl) phenol | 1.26 |
| 15 | 59.69 | 2,6-Dimethoxy-4-(2-propenyl) phenol | 0.76 |
| 16 | 73.43 | Hexadecanoic acid | 23.81 |
| 17 | 81.00; 81.41; 81.66 | Octadecadienoic acid (linoleic acid) | 39.54 |

**Table 5**
Identification and yield (area %) of aliphatic subfraction of bio-oil (pyrolysis temperature: 500 °C; heating rate: 300 °C $\min^{-1}$; $N_2$ flow rate: 200 $cm^3 \min^{-1}$).

| Peak number | Retention time (min) | Product | Relative area (%) |
|---|---|---|---|
| 1 | 11.27 | 2-Dodecene | 2.79 |
| 2 | 11.40 | Dodecane | 1.39 |
| 3 | 11.79 | Cyclodecene | 0.58 |
| 4 | 12.76 | 1-Tridecene | 3.26 |
| 5 | 12.88 | Tridecane | 2.43 |
| 6 | 14.14 | 1-Tetradecene | 8.11 |
| 7 | 14.24 | Tetradecane | 3.22 |
| 8 | 14.31 | 7-Tetradecene | 0.52 |
| 9 | 14.98 | 1,11-Dodecadiene | 0.63 |
| 10 | 15.52 | Pentadecane | 14.86 |
| 11 | 16.17 | n-Nonylcyclohexane | 1.24 |
| 12 | 16.42 | 6,8-Tetradecadiene | 1.33 |
| 13 | 16.63 | 1-Hexadecene | 2.93 |
| 14 | 16.76 | 3-Hexadecene | 4.26 |
| 15 | 16.71 | Hexadecane | 1.96 |
| 16 | 17.67 | 8-Heptadecene | 18.59 |
| 17 | 17.76 | 1-Heptadecene | 4.93 |
| 18 | 17.84 | Heptadecane | 4.20 |
| 19 | 18.19 | cis-2-Methyl-7-octadecene | 3.38 |
| 20 | 18.48 | 6,9-Heptadecadiene | 1.91 |
| 21 | 18.75 | 9-Octadecene | 1.48 |
| 22 | 18.86 | 1-Octadecene | 0.65 |
| 23 | 18.92 | Octadecane | 0.83 |
| 24 | 19.95 | Nonadecane | 0.80 |
| 25 | 20.94 | Eicosane | 1.64 |
| 26 | 21.87 | Heneicosane | 1.10 |
| 27 | 22.72 | 3-Eicosene | 1.94 |
| 28 | 23.64 | Tricosane | 0.73 |
| 29 | 26.03 | Docosane | 0.68 |
| | | *Alkanes* | 35.05 |
| | | *Alkenes* | 57.28 |

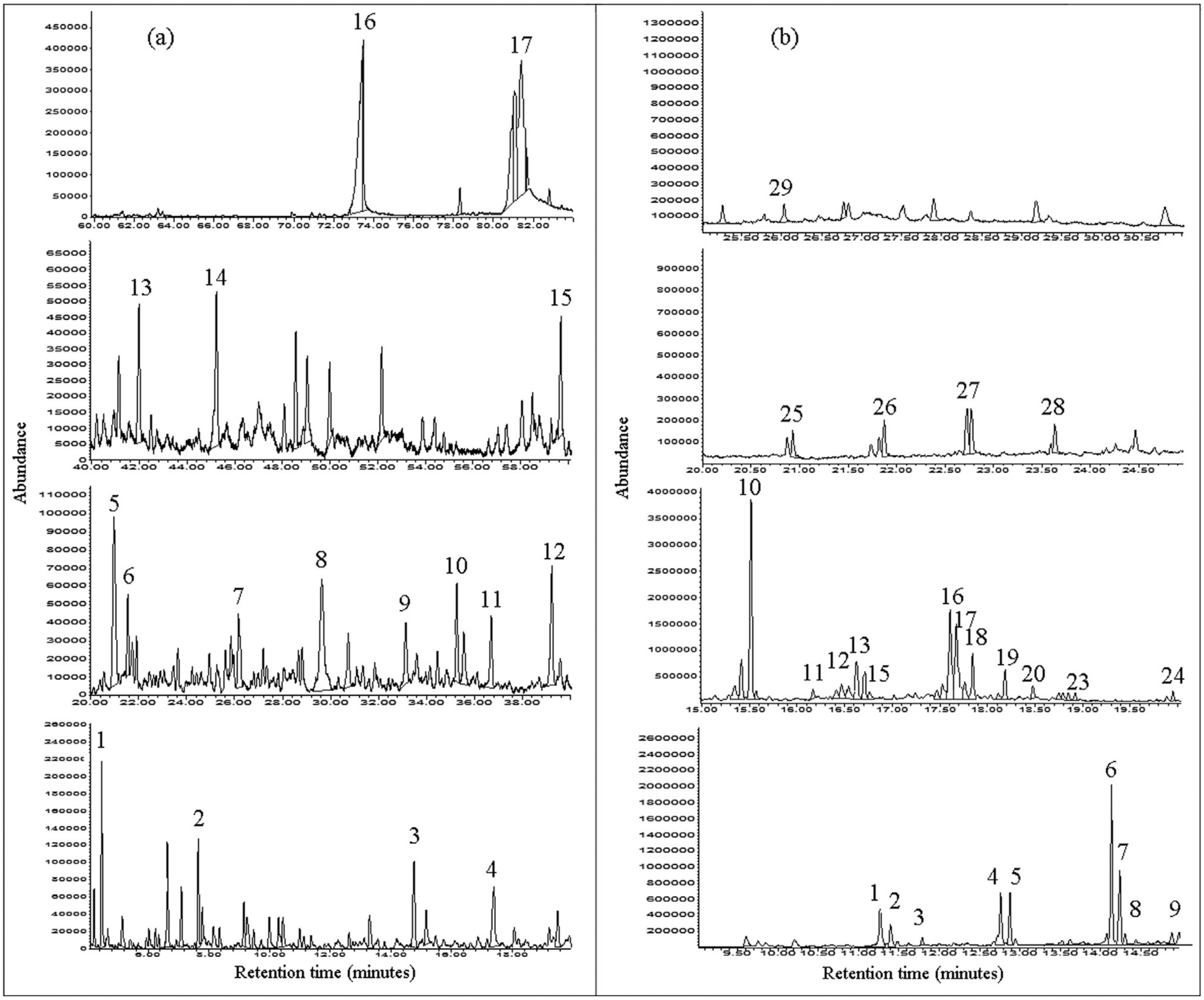

**Fig. 6.** GC–MS chromatogram of (a) bio-oil and (b) its aliphatic subfraction (peak numbers refer to tentative identification of the compounds listed in Tables 4 and 5).

acetone, pentanone, indanone and alkylated derivatives, phenol, alkylated phenols and oxyphenols, etc.

Although many analytical techniques are required to obtain a complete analysis of bio-oil, the most extensively used analyzing method for pyrolysis oils is GC/MS. Fig. 6 shows the GC/MS spectra of the bio-oil and its aliphatic sub-fraction. Peak identifications (for the peaks having area percentages greater than 0.75) that were achieved from Wiley 275 library are given in Table 4 for the bio-oil. The major compounds with 22.9 and 38 area percentages are –oic acids, mainly hexadecanoic and octadecadienoic (linoleic acid) acids respectively, that are the proof of the presence of n-hexane solubles in the raw material. In addition, aromatic hydrocarbons such as phenolics, cresols and guaiacols are observed (Table 4).

The aliphatic subfraction consists of n-alkanes, alkenes and branched hydrocarbons (Fig. 6). The majority of the linear chain hydrocarbons were distributed in the range of $C_{12}$–$C_{28}$, but the intensive peaks can be considered as $C_{11}$–$C_{18}$. In the spectrum mostly doublet peaks were observed. The first ones belong to n-alkenes and the second ones to n-alkane [45]. Table 5 gives the identification of peaks, and their retention times. According to the area percentages, it can be concluded that aliphatic subfraction is consisted of 35.05% alkanes, and 57.28% alkenes. When compared with standard diesel, it is obviously seen that the distribution of hydrocarbons for aliphatic subfraction shows similarities with conventional ones.

## 4. Conclusions

Studies on the TGA-FTIR-MS and fast pyrolysis of cottonseed and characterization of the bio-oil obtained at optimum conditions are given in this paper.

Thermal degradation characteristics and evolved gases during pyrolysis of cottonseed were analyzed by TGA-FTIR-MS. It was observed from TG and dTG curves that pyrolysis of cottonseed occurred in four zones: (i) moisture evolution, (ii) hemicellulose decomposition, (iii) cellulose and oil degradation, and (iv) lignin decomposition. Pyrolysis reactions started at 190 °C and further decelerated at the temperatures higher than 553 °C. According to consistent data obtained from FTIR and MS simultaneously, the main gases evolved are detected to be water, carbon monoxide, carbon dioxide and other light hydrocarbons and they were generated between 190 and 537 °C whereas, formation of methane lasts for 678 °C.

For the fast pyrolysis experiments, different pyrolytic conditions on product yields were examined and characteristics were found similar to those in the TGA. Pyrolysis temperature was found to be the most effective parameter among the others tried in this study. Bio-oil yield increased with the increase in temperature and gave a peak at 500 °C with 49.5% where decomposition of cottonseed was nearly completed. Sweeping gas flow rate has found to be less effective on product yields, whereas formation of gaseous products increase significantly at higher heating rates. In particular, it is recommend that when bio-oil production from cottonseed via one step thermal conversion is aimed, following conditions should be chosen to obtain maximum yields: final temperature of 500 °C, heating rate of 300 °C $\text{min}^{-1}$ and sweeping gas flow rate of 200 $\text{cm}^3\,\text{min}^{-1}$.

The bio-oil pyrolyzed from cottonseed contains high amount of oxygen. This unfavorable property was prevented by fractionating it into chemical classes (aliphatic, olefinic and polar) by column chromatography. The result of FT-IR for aliphatic subfraction is in consistency with elemental analysis, confirming that this subfraction does not contain highly oxygenated compounds like standard diesel. Further characterization of aliphatic subfraction with GC/MS showed that aliphatic subfraction is a mixture of straight chain and branched alkanes (37.96%) and alkenes (62.04%).

According to detailed characterization of oil, obtained bio-oil and its aliphatic subfraction show similarities with currently utilized transport fuels and can be considered as synthetic fuels.

## References

[1] J. Wang, M. Musamech, Y. Lin, Solubilization of carbon nanotubes by Nafion toward the preparation of amperometric biosensors, J. Am. Chem. Soc. 125 (2003) 2408–2409.
[2] H.L. Chum, R.P. Overend, Biomass and renewable fuels, Fuel Process. Technol. 71 (2001) 187–195.
[3] A.V. Brigdwater, Review of fast pyrolysis of biomass and product upgrading, Biomass Bioenergy 38 (2012) 68–94.
[4] J.F. Gonzalez, J.M. Encinar, J.L. Canito, E. Sabio, M. Chacón, Pyrolysis of cherry stones: energy uses of the different fractions and kinetic study, J. Anal. Appl. Pyrolysis 67 (2003) 165–190.
[5] H.S. Heo, H.J. Park, J.I. Dong, S.H. Park, S. Kim, D.J. Suh, Y.W. Suh, S.S. Kim, Y.K. Park, Fast pyrolysis of rice husk under different reaction conditions, J. Ind. Eng. Chem. 16 (2010) 27–31.
[6] G. Kumar, A.K. Panda, R.K. Singh, Optimization of process for the production of bio-oil from eucalyptus wood, J. Fuel Chem. Technol. 38 (2010) 162–167.
[7] E. Putun, B.B. Uzun, A.E. Putun, Production of bio-fuels from cottonseed cake by catalytic pyrolysis under steam atmosphere, Biomass Bioenergy 30 (2006) 592–598.
[8] Turkish Statistical Institute, www.turkstat.gov.tr
[9] Md.N. Nabi, Md.M. Rahman, Md.S. Akhter, Biodiesel from cottonseed oil and its effect on engine performance and exhaust emissions, Appl. Therm. Eng. 29 (2009) 2265–2270.
[10] U. Rashid, F. Anwar, G. Knothe, Evaluation of biodiesel obtained from cottonseed oil, Fuel Process. Technol. 90 (2009) 1157–1163.
[11] S.M.P. Meneghetti, M.R. Meneghetti, T.M. Serra, D.C. Barbosa, C.R. Wolf, Biodiesel production from vegetable oil mixtures: cottonseed, soybean, and castor oils, Energy Fuels 21 (2007) 3746–3747.
[12] A.V. Bridgwater, Review of fast pyrolysis of biomass and product upgrading, Biomass Bioenergy 38 (2012) 68–94.
[13] N. Jendoubia, F. Brousta, J.M. Commandre, G. Mauviel, M. Sardin, J. Lede, Inorganics distribution in bio oils and char produced by biomass fast pyrolysis: the key role of aerosols, J. Anal. Appl. Pyrolysis 92 (2011) 59–67.
[14] N. Ozbay, E. Apaydın-Varol, B.B. Uzun, A.E. Putun, Characterization of bio-oil obtained from fruit pulp pyrolysis, Energy 33 (2008) 1233–1240.
[15] A.W. Schwab, G.J. Dykstra, E. Selke, S.C. Sorenson, E.H. Pryde, Diesel fuel from thermal decomposition of soybean oil, J. Am. Oil Chem. Soc. 65 (1988) 1781–1786.
[16] J.W. Alencar, P.B. Alves, A.A. Craveiro, Pyrolysis of tropical vegetable oils, J. Agric. Food Chem. 31 (1983) 1268–1270.
[17] D.G. Lima, V.C.D. Soares, E.B. Ribeiro, D.A. Carvalho, É.C.V. Cardoso, F.C. Rassi, K.C. Mundima, J.C. Rubima, P.A.Z. Suarez, Diesel-like fuel obtained by pyrolysis of vegetable oils, J. Anal. Appl. Pyrolysis 71 (2004) 987–996.
[18] R.O. Idem, S.P.R. Katikaneni, N.N. Bakhshi, Thermal cracking of canola oil: reaction products in the presence and absence of steam, Energy Fuels 10 (1996) 1150–1162.
[19] H. Li, P. Yu, B. Shen, Biofuel potential production from cottonseed oil: a comparison of non-catalytic and catalytic pyrolysis on fixed-fluidized bed reactor, Fuel Process. Technol. 90 (2009) 1087–1092.
[20] N. Özbay, A.E. Pütün, B.B. Uzun, E. Pütün, Biocrude from biomass: pyrolysis of cottonseed cake, Renew. Energ. 24 (2001) 615–625.
[21] E. Putun, B.B. Uzun, A.E. Putun, Fixed-bed catalytic pyrolysis of cotton-seed cake: effects of pyrolysis temperature, natural zeolite content and sweeping gas flow rate, Bioresour. Technol. 97 (2006) 701–710.
[22] E. Pütün, Catalytic pyrolysis of biomass: effects of pyrolysis temperature, sweeping gas flow rate and MgO catalyst, Energy 35 (2010) 2761–2766.
[23] J.E. White, W.J. Catallo, B.L. Legendre, Biomass pyrolysis kinetics: a comparative critical review with relevant agricultural residue case studies, J. Anal. Appl. Pyrolysis 91 (2011) 1–33.
[24] L. Burhenne, J. Messmer, T. Aicher, M.P. Laborie, The effect of the biomass components lignin, cellulose and hemicellulose on TGA and fixed bed pyrolysis, J. Anal. Appl. Pyrolysis 101 (2013) 177–184.
[25] D.K. Seo, S.S. Park, J. Hwang, T.U. Yub, Study of the pyrolysis of biomass using thermo-gravimetric analysis (TGA) and concentration measurements of the evolved species, J. Anal. Appl. Pyrolysis 89 (2010) 66–73.
[26] D. Chen, Y. Zheng, X. Zhu, In-depth investigation on the pyrolysis kinetics of raw biomass. Part I: kinetic analysis for the drying and devolatilization stages, Bioresour. Technol. 131 (2013) 40–46.
[27] M. Zhang, F.L.P. Resende, A. Moutsoglou, D.E. Rayniec, Pyrolysis of lignin extracted from prairie cordgrass, aspen, and Kraft lignin by Py-GC/MS and TGA/FTIR, J. Anal. Appl. Pyrolysis 98 (2012) 65–71.
[28] T. Damartzis, D. Vamvuka, S. Sfakiotakis, A. Zabaniotou, Thermal degradation studies and kinetic modeling of cardoon (*Cynara cardunculus*) pyrolysis using thermogravimetric analysis (TGA), Bioresour. Technol. 102 (2011) 6230–6238.
[29] L. Sanchez-Silva, D. López-González, J. Villaseñor, P. Sánchez, J.L. Valverde, Thermogravimetric-mass spectrometric analysis of lignocellulosic and marine biomass pyrolysis, Bioresour. Technol. 109 (2012) 163–172.
[30] S. Singh, C. Wu, P.T. Williams, Pyrolysis of waste materials using TGA-MS and TGA-FTIR as complementary characterisation techniques, J. Anal. Appl. Pyrolysis 94 (2012) 99–107.
[31] Q. Ren, C. Zhao, X. Wu, C. Liang, X. Chen, J. Shen, G. Tang, Z. Wang, TG-FTIR study on co-pyrolysis of municipal solid waste with biomass, Bioresour. Technol. 100 (2009) 4054–4057.
[32] J.H. Harker, J.R. Backhurst, Fuel and Energy, Academic Press Limited, London, 1981.
[33] B.B. Uzun, A.E. Pütün, E. Pütün, Rapid pyrolysis of olive residue. 1. Effect of heat and mass transfer limitations on product yields and bio-oil compositions, Energy Fuels 21 (3) (2007) 1768–1776.
[34] A.E. Pütün, B.B. Uzun, E. Apaydin, E. Pütün, Bio-oil from olive oil industry wastes: pyrolysis of olive residue under different conditions, Fuel Process. Technol. 87 (2005) 25–32.
[35] B.B. Uzun, E. Apaydin-Varol, F. Ateş, N. Özbay, A.E. Pütün, Synthetic fuel production from tea waste: characterisation of bio-oil and bio-char, Fuel 89 (2010) 176–184.
[36] G. Duman, C. Okutucu, S. Ucar, R. Stahl, J. Yanik, The slow and fast pyrolysis of cherry seed, Bioresour. Technol. 102 (2011) 1869–1878.
[37] E. Apaydin-Varol, E. Pütün, A.E. Pütün, Slow pyrolysis of pistachio shell, Fuel 86 (2007) 1892–1899.
[38] F. Abnisa, W.M.A. Wan Daud, W.N.W. Husin, J.N. Sahu, Utilization possibilities of palm shell as a source of biomass energy in Malaysia by producing bio-oil in pyrolysis process, Biomass Bioenergy 35 (2011) 1863–1872.
[39] W. Li, Z. Zhou, Y. Meng, N. Xu, M. Fok, Modeling boll maturation period, seed growth, protein, and oil content of cotton (*Gossypium hirsutum* L.) in China, Field Crops Res. 112 (2009) 131–140.
[40] A.V. Bridgwater, G.V.C. Peacocke, Fast pyrolysis processes for biomass, Renew. Sustain. Energy Rev. 4 (2000) 1–73.
[41] F. Rick, U. Vix, Product standards for pyrolysis products for use as fuel in industrial firing plants, in: A.V. Bridgwater, G. Grassi (Eds.), Biomass Pyrolysis Liquids Upgrading and Utilization, Elsevier Science, London, 1991, pp. 177–218.
[42] R.G. Andrews, P.C. Patniak, Feasibility of utilizing a biomass derived fuel for industrial gas turbine application, in: A.V. Bridgwater, E.N. Hogon (Eds.), Bio-oil Production and Utilization, CPL Press, Berkshire, 1997, pp. 236–245.
[43] W.T. Tsai, M.K. Lee, Y.M. Chang, Fast pyrolysis of rice straw, sugarcane bagasse and coconut shell in an induction-heating reactor, J. Anal. Appl. Pyrolysis 76 (2006) 230–237.
[44] Z. Wang, J. Cao, J. Wang, Pyrolytic characteristics of pine wood in a slowly heating and gas sweeping fixed-bed reactor, J. Anal. Appl. Pyrolysis 84 (2009) 179–184.
[45] R.V. Pindoria, J.Y. Lim, J.E. Hawkes, M.J. Lazaro, A.A. Herod, R. Kandioti, Structural characterization of biomass pyrolysis tars/oils from eucalyptus wood waste: effect of $H_2$ pressure and sample configuration, Fuel 76 (1997) 1013–1023.